

Supporting Information

Enhanced phosphate sequestration by Fe(III) modified biochar derived from coconut shell

Zhenxing Zhong¹, Guowen Yu¹, Wenting Mo², Chunjie Zhang¹, Hao Huang^{1,3}, Shengui Li², Meng Gao⁴, Xiejuan Lu^{1*}, Beiping Zhang¹, Hongping Zhu⁵

¹ School of Environmental Science and Engineering, Huazhong University of Science and Technology, Wuhan 430074, China

² Department of Urban Construction, Wuchang Shouyi University, Wuhan, 430064, China

³ Wuhan Planning and Design Company, Wuhan, 430014, China

⁴ Huangshi Institute of Environmental Protection, Huangshi, 435000, China

⁵School of Civil Engineering & Mechanics, Huazhong University of Science and Technology, Wuhan 430074, China

*Corresponding author: luxiejuanhust@163.com (X.J Lu); Tel: +27-87792155

Appendix A

Table S1 List of isotherm models and kinetic models in this study

Kinetic models [1]	Parameters	Isotherm models [2]	Parameters
First-order: $\frac{dq_t}{dt} = k_1(q_e - q_t)$ $q_e, q_t, k_1, R^2;$ $\ln(q_e - q_t) = \ln q_e - k_1 t$		Freundlich $q_e = K_f C_e^{1/n}$	$K_f, n, R^2;$
Second-order: $\frac{dq_t}{dt} = k_2(q_e - q_t)^2$ $q_e, q_t, k_2, R^2;$ $\frac{t}{q_t} = \frac{1}{k_2 q_e^2} + \frac{t}{q_e}$		Langmuir $q_e = \frac{K_l q_m C_e}{1 + K C_e}$	$K_l, q_m, R^2;$
Richie n-th-order: $\frac{dq_t}{dt} = k_n(q_e - q_t)^n$ $q_e, q_t, k_n,$ $n, R^2;$ $q_t = q_e - ((n-1)k_n t + q_e^{1-n})^{\frac{1}{1-n}}$		Langmuir- Freundlich $q_e = \frac{K_{lf} q_m C_e^n}{1 + K_{lf} C_e^n}$	$K_{lf}, q_m, n, R^2;$
Elovich: $\frac{dq_t}{dt} = a \exp(-b q_t)$ $q_t = \frac{1}{b} \ln(abt + 1)$	a, b, q_t, R^2		

Table S2 Kinetic parameters of phosphate sorption to CSBs based on the intra-particle diffusion model [3]

Adsorbents	K_{p1} (mg/g•h ^{1/2})	C_1 (mg/g)	R^2	K_{p2} (mg/g•h ^{1/2})	C_2 (mg/g)	R^2
CSB	1.023	0.463	0.797	0.049	1.886	0.895
Fe-CSB	0.806	1.212	0.905	0.323	2.092	0.923

The intraparticle diffusion model: $q_t = k_p \cdot t^{1/2} + C$, where K_p is the intraparticle diffusion rate constant (mg/g•h^{1/2}), and C is a constant that reflects the thickness of the boundary layer.

Table S3 Thermodynamic parameters of P adsorption for CSB and Fe-CSB

Materials	T (K)	Parameters			
		K ₀ (L/mg)	ΔG ⁰ (kJ/mol)	ΔH ⁰ (kJ/mol)	ΔS ⁰ (J/mol/K)
CSB	298	0.13	-12.06		
	308	0.15	-12.82	21.58	111.43
	318	0.20	-14.01		
Fe-CSB	298	1.43	-18.00		
	308	1.54	-18.79	26.54	82.11
	318	1.63	-19.56		

Thermodynamic parameters are determined by the following equations [4]:

$$K_0 = \frac{q_e}{C_e} \quad (1); \quad \Delta G = -RT \ln K_0 \quad (2); \quad \Delta G = \Delta H - T\Delta S^0 \quad (3); \quad \ln K_0 = \frac{\Delta H^0}{RT} - \frac{\Delta S^0}{R} \quad (4);$$

where K₀ is the adsorption coefficient, R is gas constant (kJ/mol K), and T is the absolute temperature (K), respectively.

Table S4 Comparison of maximum P sorption capacities for various Fe-based materials

Adsorbents	Solution pH	Contact time (h)	Temperature (°C)	Fe (wt %)	Equilibrium Ce (mg/g)	Max q _m (mg/g)	Ref.
Fe-CSB	7.0	24	25	11.2%	2-100	36.0	This work
Fe(III)-Bentonite	7.0	96	25	2.78%	0.05-5.0	11.2	[5]
Granulated ferric hydroxide	5.5	24	20	31.4%	0.3-4.0	23.3	[6]
Magnetic water hyacinth biochar	7.0	24	25	15.0-27.1%	0.2-150	5.1	[7]
Fe-impregnated woodchip biochar	5.6	24	24	2-4%	10-200	3.2	[8]
Fe-doped activated carbon	7.0	24	RT ^a	18.6%	15-640	8.1	[9]
Fe ³⁺ /Fe ²⁺ modified WAS biochar	7.0	2	22	24.2%	5-1000	34.2	[10]
Magnetic Fe-Zr binary oxide	4.0	24	25	26.62%	0-100	13.7	[11]
Ferrihydrite	7.0	24	25	31.4%	0-250	22.2	[12]

a: RT, room temperature;

Table S5 Chemical reactions between phosphate and metal ions in this study

Solid formed	Chemical equation	Solubility equation constant ($\log K$)	Ref.
Ferric phosphate	$\text{Fe}^{3+} + \text{PO}_3^{-} \rightleftharpoons \text{FePO}_{4(\text{s})}$	21.9	[13]
Iron (III) hydrogen phosphate	$2\text{Fe}^{3+} + 3\text{HPO}_2^{-} \rightleftharpoons \text{Fe}_2(\text{HPO}_4)_{3(\text{s})}$	30.9	[14]
Iron (II) dihydrogen phosphate	$\text{Fe}^{3+} + 3\text{H}_2\text{PO}^{-} \rightleftharpoons \text{Fe}(\text{H}_2\text{PO}_4)_{3(\text{s})}$	26.6	[14]
Aluminum phosphate	$\text{Al}^{3+} + \text{PO}_3^{-} \rightleftharpoons \text{AlPO}_{4(\text{s})}$	21.0	[13]
Aluminum hydrogen phosphate	$2\text{Al}^{3+} + 3\text{HPO}_2^{-} \rightleftharpoons \text{Al}_2(\text{HPO}_4)_{3(\text{s})}$	Particles	[15]
Calcium hydrogen phosphate	$\text{Ca}^{2+} + \text{HPO}_2^{-} \rightleftharpoons \text{CaHPO}_{4(\text{s})}$	6.66	[16]
Calcium dihydrogen phosphate	$\text{Ca}^{2+} + 2\text{H}_2\text{PO}^{-} \rightleftharpoons \text{Ca}(\text{H}_2\text{PO}_4)_{2(\text{s})}$	1.14	[16]
Tricalcium phosphate	$3\text{Ca}^{2+} + 2\text{PO}_3^{-} \rightleftharpoons \text{Ca}_3(\text{PO}_4)_{2(\text{s})}$	24.0	[16]
Hydroxyapatite	$5\text{Ca}^{2+} + 3\text{PO}_3^{-} + \text{OH}^{-} \rightleftharpoons \text{Ca}_5(\text{PO}_4)_3\text{OH}_{(\text{s})}$	55.9	[16]
Magnesium phosphate	$3\text{Mg}^{2+} + 2\text{PO}_3^{-} \rightleftharpoons \text{Mg}_3(\text{PO}_4)_{2(\text{s})}$	25.2	[1]
Magnesium hydrogen phosphate	$\text{Mg}^{2+} + \text{HPO}_2^{-} \rightleftharpoons \text{MgHPO}_{4(\text{s})}$	5.82	[1]
Magnesium dihydrogen phosphate	$\text{Mg}^{2+} + 2\text{H}_2\text{PO}^{-} \rightleftharpoons \text{Mg}(\text{H}_2\text{PO}_4)_{2(\text{s})}$	Particles	[1]

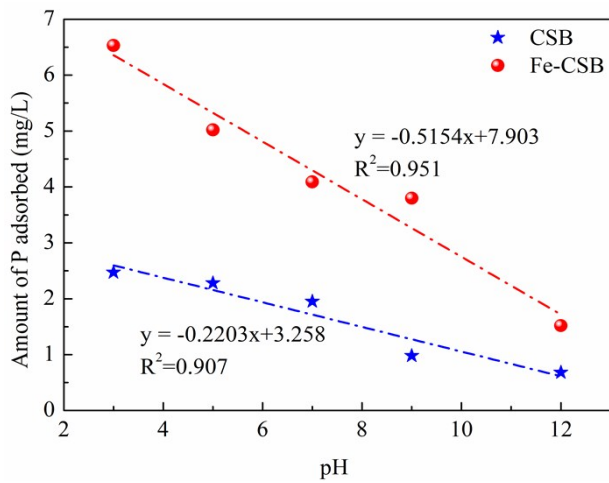


Fig. S1 Linear correlations between the initial pH and the P adsorption amount of CSB and Fe-CSB

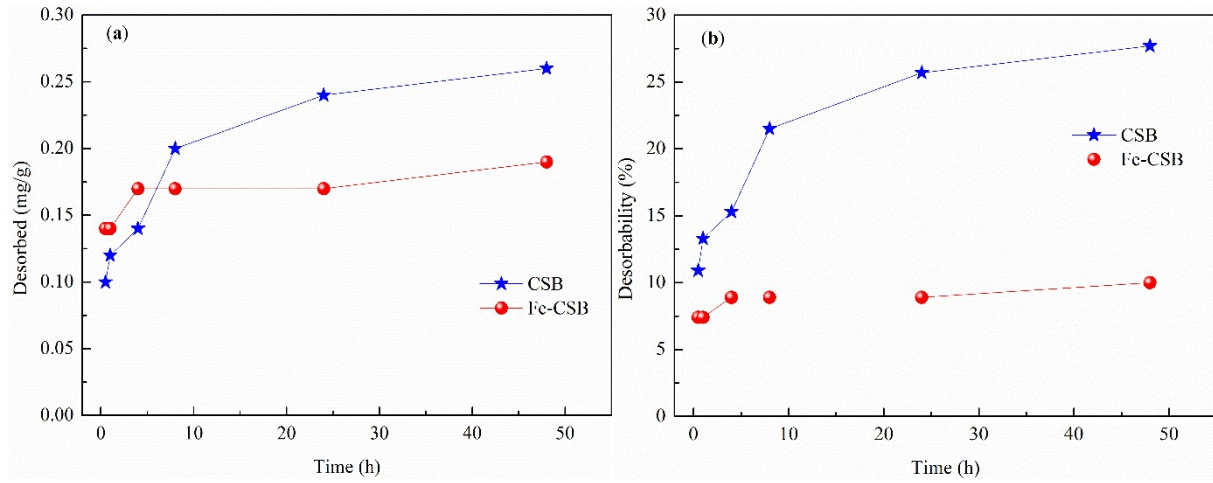


Fig. S2 Desorbed amount (a) and Desorbability (b) of the adsorbed P from the CSB and Fe-CSB

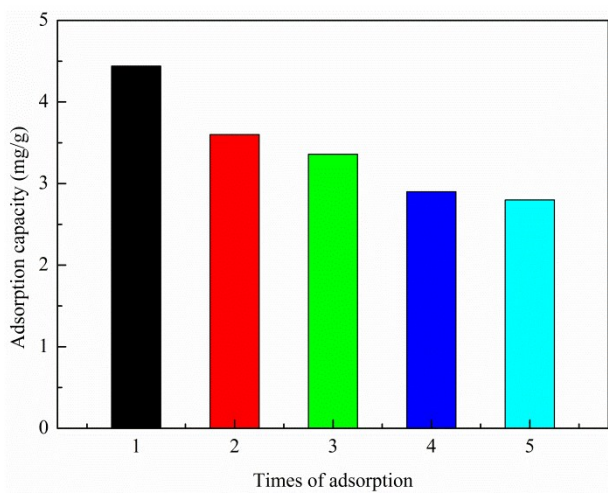


Fig. S3. The adsorption capacity of phosphate by Fe-CSB during five successive cycles

References:

1. Y. Yao, B. Gao, J. Chen, L. Yang, *Environ Sci Technol*, 2013, 47, 8700-8708.
2. L. Zeng, X. Li, J. Liu, *Water Research*, 2004, 38, 1318-1326.
3. V Kuroki, G E. Bosco, P S. Fadini, *Journal of Hazardous Materials*, 2014, 274, 124–131.
4. P. Liao, S. Yuan, W. Xie, W. Zhang, M. Tong, K. Wang, *Journal of Colloid and Interface Science*, 2013, 390, 189-195.
5. M. Zamparas, A. Gianni, P. Stathi, Y. Deligiannakis, I. Zacharias, *Applied Clay Science*, 2012, 62–63, 101–106.
6. A. Genz, A. Kornmuller, M. Jekel, Advanced phosphorus removal from membrane filtrates by adsorption on activated aluminium oxide and granulated ferric hydroxide, *Water Research*, 38 (2004) 3523–3530.
7. R. Cai, X. Wang, X.H Ji, B. Peng, C.Y. Tan, X. Huang, *Journal of Environmental Management*, 2017, 187, 212-219.
8. B. Micháleková-Richveisová, V. Frišták, M. Pipíška, L. Ďuriška, E. Moreno-Jimenez, G. Soja, *Environ Sci Pollut Res*, 2017, 24, 463–475.
9. Y. Yao, B. Gao, M. Inyang, A. R. Zimmerman, X.D Cao, P. Pullammanappallil, L.Y. Yang, *Journal of Hazardous Materials*, 2011, 190, 501–507.
10. Q. Yang, X.L. Wang, W. Luo, J. Sun, *Bioresource Technology*, 2018, 247, 537–544.
11. F. Long, J.-L. Gong, G.-M. Zeng, L. Chen, X.-Y. Wang, J.-H. Deng, Q.-Y. Niu, H.-Y. Zhang, X.-R. Zhang, *Chemical Engineering Journal*, 2011, 171, 448-455.
12. J. Yan, T. Jiang, Y. Yao, S. Lu, Q. Wang, S. Wei, *Journal of Environmental Sciences*, 2016, 42, 152-162.
13. G W Yu, B P Zhang, X J Lu, *Arab J Geosci*, 2015, 8, 3491–3499.
14. D. Rich, [D], Northwestern International University, 2005.
15. H R Liu, W L Jiang, G M Su, *Modern Paint & Finishing*, 2010, 13, 10-12 (Chinese).
16. T Hiemstra, J Antelo, R Rahnemaie, *Geochimica et Cosmochimica Acta*, 2010, 74, 41–58.